Available online at www.sciencedirect.com
ScienceDirect
Journal of Magnetic Resonance 192 (2008) 167–172
JMR Journal of Magnetic Resonance
www.elsevier.com/locate/jmr

Communication

High-performance solvent suppression for proton detected solid-state NMR

Donghua H. Zhou [a], Chad M. Rienstra [a,b,c,*]

[a] Department of Chemistry, University of Illinois at Urbana-Champaign, Urbana, IL 61801, USA
[b] Department of Biochemistry, University of Illinois at Urbana-Champaign, Urbana, IL 61801, USA
[c] Center for Biophysics and Computational Biology, University of Illinois at Urbana-Champaign, Urbana, IL 61801, USA

Received 5 November 2007; revised 23 January 2008
Available online 1 February 2008

Abstract

High-sensitivity proton detected experiments in solid-state NMR have been recently demonstrated in proton diluted proteins as well as fully protonated samples under fast magic-angle spinning. One key element for performing successful proton detection is effective solvent suppression achieved by pulsed field gradients (PFG) and/or saturation pulses. Here we report a high-performance solvent suppression method that attenuates multiple solvent signals simultaneously by more than a factor of 10,000, achieved by an optimized combination of homospoil gradients and supercycled saturation pulses. This method, which we call Multiple Intense Solvent Suppression Intended for Sensitive Spectroscopic Investigation of Protonated Proteins, Instantly (MISSISSIPPI), can be applied without a PFG probe. It opens up new opportunities for two-dimensional heteronuclear correlation spectroscopy of hydrated proteins at *natural abundance* as well as high-sensitivity and multi-dimensional experimental investigation of protein–solvent interactions.

Keywords: Solvent suppression; Proton detection; Natural abundance; Protein–solvent interactions; Magic-angle spinning NMR

1. Introduction

Magic-angle spinning solid-state NMR (MAS SSNMR) has been demonstrated as a powerful tool for protein structure determination and the investigation of protein–solvent interactions [1–7]. However, the majority of experiments so far have been performed by detecting on either ^{13}C or ^{15}N nuclei, which are relatively insensitive due to their low gyromagnetic ratios. High-sensitivity detection on ^{1}H has only been realized recently in SSNMR. The strong proton dipolar coupling problem has been addressed with two approaches: (1) diluting the proton bath, (2) spinning fully protonated samples at ~40 kHz. The first approach yields very high-resolution [8–11] and ^{1}H–^{1}H distance restraints as long as 9 Å have been detected, enabling the determination of a high-resolution protein structure [12]. The second approach is important for systems such as membrane proteins where deuteration and back-exchange may be challenging; it also permits all non-exchangeable protons to be investigated in a single experiment [13]. Both approaches result in a common outcome of greatly enhanced sensitivity relative to ^{13}C or ^{15}N detection.

To utilize this enhanced detection sensitivity for analyses of natural abundance proteins is one important application of these developments. Our initial attempts to perform fast MAS proton detection heteronuclear correlation (HETCOR) experiments on natural abundance proteins, however, were unsuccessful due to the overwhelming solvent signal intensity. In hydrated protein samples containing roughly 1 μmol of protein and 1 μL of water, the ratio of water to protein signal is 100, and the protein signal will be at least ~100 (or 270) times weaker when performing correlation experiments with ^{13}C (or ^{15}N) at natural

* Corresponding author. Address: Department of Chemistry, University of Illinois at Urbana-Champaign, Urbana, IL 61801, USA. Fax: +1 217 244 3186.
E-mail address: Rienstra@scs.uiuc.edu (C.M. Rienstra).

1090-7807/$ - see front matter © 2008 Elsevier Inc. All rights reserved.
doi:10.1016/j.jmr.2008.01.012

abundance. Therefore the water resonance is more than 10,000 times stronger than a ^{13}C or ^{15}N-edited protein proton resonance; thus water and other solvent signals must be suppressed by four orders of magnitude to utilize the full receiver dynamic range for the protein signals. Previously reported solvent suppression schemes yield suppression by two to three orders of magnitude for a single resonance line (such as water), achieved by employing either pulsed field gradients (PFGs) [9] or saturation pulses [10]. We had extended the method of Paulson and Zilm [10] to achieve simultaneous suppression of multiple solvent signals, by using a long, moderate-power saturation pulse [13]. Here we report a new high-performance suppression method, which we call Multiple Intense Solvent Suppression Intended for Sensitive Spectroscopic Investigation of Protonated Proteins, Instantly (MISSISSIPPI). This approach combines both gradient and saturation pulses. Since pulsed field gradients are generally not available for all types of solid-state NMR probes, we substitute with homospoil gradients, in which case the Z_1 shimming current is maximized for a short duration to apply a small gradient (a few Gauss per centimeter). MISSISSIPPI employs carefully ordered homospoil gradients and saturation pulses with supercycled phases, resulting in attenuation of multiple solvent signals simultaneously by at least a factor of 10,000, opening up new opportunities for spectroscopy of natural abundance proteins and investigation of protein–solvent interactions.

2. Experimental

Natural abundance and ^{2}H, ^{13}C, ^{15}N-labeled β1 immunoglobulin binding domain of protein G (GB1) were prepared according to previously published procedures [12,14]. Nanocrystalline GB1 samples were precipitated with natural abundance 2-methyl-pentane-2,4-diol (MPD) and isopropanol (IPA) [14]. About 5 mg (0.9 μmol) GB1 and 4 mg solvents were packed into the 1.6-mm MAS rotor, with a rubber disc on each end to maintain hydration [13].

The SSNMR experiments were performed on a 750 MHz Varian INOVA spectrometer with a FastMAS™ probe (Varian, Inc., Palo Alto, CA and Fort Collins, CO). The ^{1}H, ^{13}C and ^{15}N π/2 pulse widths were 1.6, 2.3 and 3.3 μs with 111, 213 and 295 W input power levels, respectively. Shimming was performed on the water signal of a 50 mM phosphorus buffer to obtain 22 Hz (0.03 ppm) ^{1}H line width. Temperature was regulated with variable temperature gas (dry air) at a set point of −5 °C with 75 scfh flow. The sample temperature was calibrated using ethylene glycol [15] and determined to be 7.2 and 10.0 °C for MAS rates (ν_R) of 36 and 39 kHz, respectively. During cross polarization (CP) [16,17], the ^{1}H and ^{15}N nutation frequencies are 2.5 and 1.5 times the MAS rate, respectively. For n.a. GB1, contact times of 1.6 and 0.6 ms were used for the ^{1}H to ^{15}N and ^{15}N to ^{1}H CP steps, respectively; for ^{2}H, ^{13}C, ^{15}N-GB1 the corresponding contact times were 1.4 and 0.3 ms. Low power XiX decoupling (nutation frequency ~10 kHz, pulse width $5.85/\nu_R$) was applied during ^{15}N evolution [18]. WALTZ-16 decoupling (6.4 kHz) was applied on ^{15}N channel during proton acquisition [10,19]. Recycle delay was 1.5 s unless specified differently. Other experimental details can be found in Section 3.1 and figure captions.

3. Results and discussion

3.1. Solvent suppression

Fig. 1 shows the MISSISSIPPI scheme in the context of a ^{15}N–^{1}H HETCOR experiment. In the beginning of the recycle delay, a homospoil pulse is turned on for τ_H to suppress transverse signals left from the previous scan. After the recycle delay, a π/2 pulse excites the ^{1}H magnetization, which is then transferred to ^{15}N by CP. After t_1 evolution, the magnetization is restored to the longitudinal axis by a ^{15}N π/2 pulse, followed by a delay t_{1max}–t_1 to maintain a constant duty cycle. A second homospoil pulse is then applied to dephase solvent signals; the parasitic eddy current (caused by the switching of the shimming current) is allowed to decay during τ_w. Proton saturation pulses are then applied for τ_S for further suppression. The magnetization is flipped to the transverse plane by a ^{15}N π/2 pulse and transferred to ^{1}H via a second CP for data acquisition. Optionally spin-diffusion or radio frequency-driven dipolar recoupling (RFDR) can be applied before acquisition in order to establish correlations among protein signals or between protein and solvent signals [20].

Each of the homospoil pulses was applied for $\tau_H = 20$ ms, the maximum allowed by the INOVA system. The delay $\tau_w > 40$ ms is needed for good suppression and

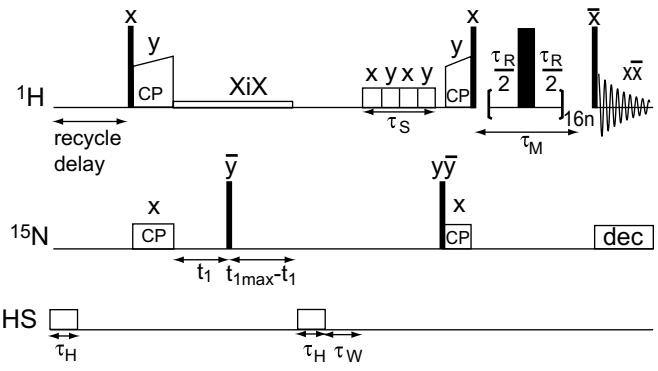

Fig. 1. MISSISSIPPI-based solid-state ^{15}N–^{1}H heteronuclear correlation pulse sequence employing homospoil gradients and saturation pulses for efficient suppression of multiple solvent signals. Optionally, RFDR (the π pulse train and bracketing π/2 pulses on ^{1}H channel) or spin-diffusion (omitting the π pulses) can be used to study protein–solvent interactions as well as proton–proton distance constraints within the protein [12,20]. For 2D acquisition, States-TPPI phase increment was applied to the π/2 pulse immediately following t_1 [23,24]. XY-16 phases [25] are used for RFDR pulses; other phases are labeled above the pulses. Narrow and wide filled rectangles represent π/2 and π pulses, respectively.

50 ms was used for data presented subsequently in this report. The RF saturation pulses should exceed a nutation frequency of 20 kHz. For best suppression performance here, we found it necessary to place these saturation pulses as late in the pulse sequence as possible. In our earlier implementation, the saturation pulse precedes any evolution periods to avoid potentially unwanted ^{15}N–^{15}N or ^{13}C–^{13}C recoupling [13]. This is not a concern with natural abundance samples, and even with ^{15}N-labeled samples, the nutation frequency can be set to the $n = 1$ DARR condition (ν_R) [21] without resulting in significant ^{15}N–^{15}N mixing, since this process is extremely slow at such high-MAS rates; we confirmed this expectation with 2D ^{15}N–^{1}H spectra of ^{2}H, ^{13}C, ^{15}N-GB1 (data not shown). For the ^{13}C–^{1}H correlation experiments on uniformly ^{13}C-labeled samples, it is best to avoid the DARR [21] conditions; setting the presaturation pulses to 0.75 ν_R for 250 ms resulted in only modest recoupling of a very small number of signals (Thr C^{β}–C^{γ} and Lys C^{β}–C^{γ} and C^{γ}–C^{δ}), as determined on a uniformly-^{13}C, ^{15}N sample of GB1 (data not shown).

Saturation pulses can be applied for a total duration of 100–300 ms; 200 ms was used for subsequent data. An even number of saturation pulses with alternating x and y phases were found to perform far better than a single pulse with the same total duration; this is an extension of the method of two pulses (400 μs each with orthogonal phases) used by Ishii to filter out protons attached to ^{12}C [22]. Two and four pulses were found appropriate for 100 and 200 ms, respectively; both four and six pulses had similar performance for $\tau_S = 300$ ms. As we reported earlier [13], the relatively long delay ($\tau_H + \tau_w + \tau_S$) is short compared to the T_1 relaxation times of ^{15}N and therefore causes very little decay. For ^{13}C, T_1 values may in general be shorter (especially for methyl groups). Although we still found only a ~10% loss over this duration, this issue should be considered when storing magnetization on ^{13}C sites. The exact proton transmitter frequency is not critical for MISSISSIPPI; the typical placement in our studies was 3 ppm.

Fig. 2 demonstrates the MISSISSIPPI results on a natural abundance GB1 sample. The solvent signals from water, MPD and IPA dominate the single pulse excitation spectrum (Fig. 2a). The weak amide proton signals are greatly attenuated in the ^{15}N-edited spectra (Fig. 2b–f) due to the low ^{15}N natural abundance (0.368%). For 2 transients (Fig. 2b), the water signal is well suppressed (by 7800 times) but the methyl signals (suppressed by 2200) are still stronger than the amide signals. The suppression efficiencies improve significantly upon signal averaging with multiple scans. Water and methyl signals are suppressed by 10,300 and 3600 times for 4 transients, respectively; 12,000 and 6900 for 8 transients; 18,800 and 13,000 for 16 transients (Fig. 2c); and 22,500 and 13,500 for 32 transients. The suppression factors are accurate when the residual solvent signals are much stronger than the noise level. In cases where the solvent signals are close to noise level, the strongest intensity in the expected solvent resonance region is used as the residual solvent intensity, leading to an *underestimate* of the suppression efficiency. While the values are not very precise in these cases, the large differences observed between different numbers of transients are reproducible and reliable. Both suppression efficiencies and signal-to-noise ratios can be further increased by truncating the time domain signal to $4T_2$ ($T_2 = 0.85$ ms for amide proton spin–spin relaxation time), which rejects the late portion of the free induction decay that contains little amide but noise and solvent signals

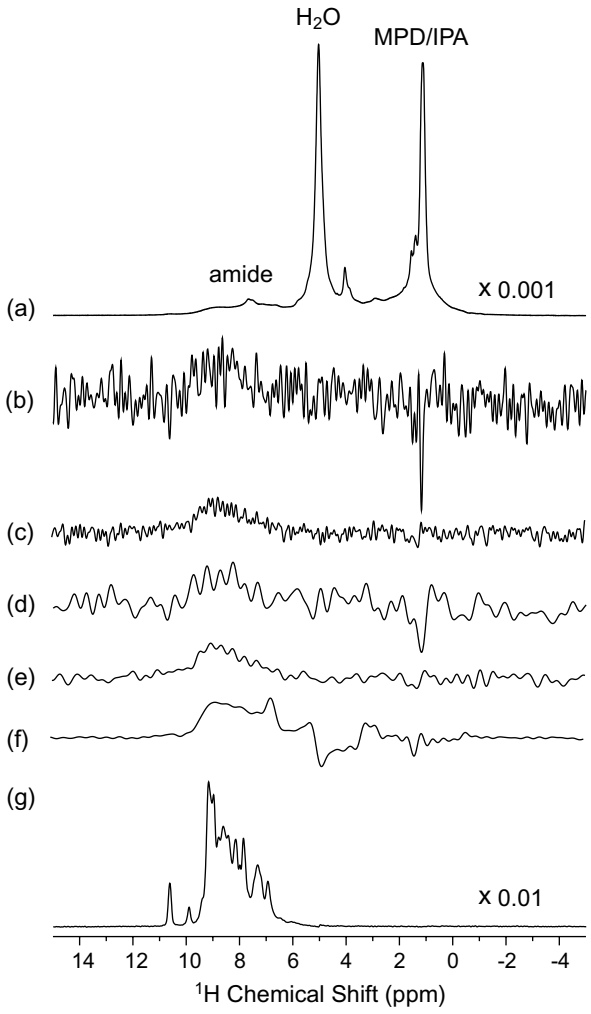

Fig. 2. Proton spectra demonstrating the solvent suppression efficiency of MISSISSIPPI. (a) Spectrum excited by a single π/2 pulse. (b–e) Spectra with MISSISSIPPI suppression and ^{15}N-editing. Two transients for (a), (b) and (d) and 16 transients for (c) and (e) were acquired. The 10 ms free induction decays in (b) and (c) were truncated to 3.4 ms for (d) and (e), respectively. (f) For comparison, a 256-transient spectrum was acquired using a previous solvent suppression method [13], also truncated to 3.4 ms. Spectra (a–f) were acquired on a 750 MHz spectrometer with 36 kHz sample spinning rate, for 0.9 μmol natural abundance nanocrystalline protein GB1 precipitated with methyl-2,4-pentanediol and isopropanol. (g) For another comparison, a 4-transient spectrum was acquired using MISSISSIPPI on a GB1 sample uniformly ^{2}H, ^{13}C, ^{15}N-enriched, back-exchanged with H_2O; free induction decay evolved to 14 ms. No apodization was applied to any spectra and intensity per transient is plotted for all spectra.

(Fig. 2d and e). For comparison, even after 256 transients of signal averaging, our previous suppression method employing a single saturation pulse (250 ms, 40 kHz) [13], which was adequate for enriched samples, resulted in strong residual solvent signals that severely interfere with amide signals of natural abundance GB1. For enriched samples, residual solvent signals after MISSISSIPPI suppression can be completely ignored with the protein signals 273 times stronger than in natural abundance samples (Fig. 2g; identical to the first spectrum of Fig. 3a).

The two-step phase cycle allows residual solvent signals to be subtracted between two scans and meanwhile the desired signals to be added; increasing phase steps has not been effective. Amplifier and probe instabilities, phase errors and quadrature gain and phase imbalance of the receiver account for the remaining solvent intensities in two scans. The observed improvement with increasing signal averaging is likely due to the apparent incoherence of the remaining solvent signals after every two scans. We attribute the better suppression for water than for solvent methyl protons to the relative T_2 values (4.7 and 13.7 ms for water and methyl, respectively).

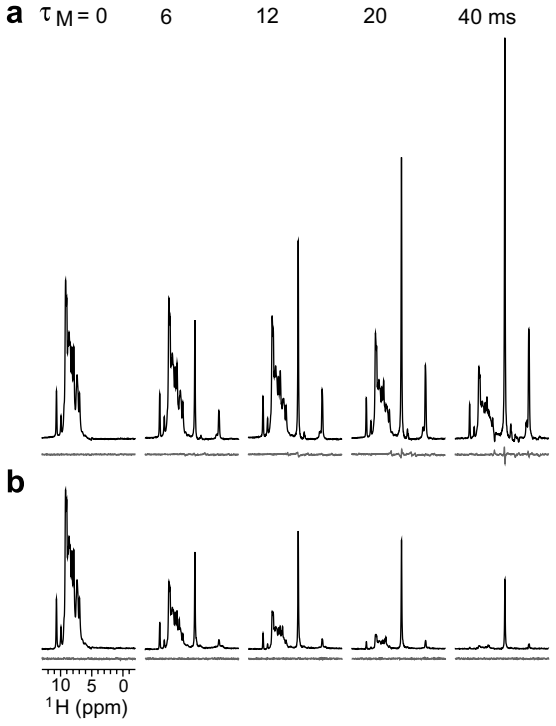

Fig. 3. The investigation of protein–solvent interactions through high-sensitivity proton detection. ^{15}N-edited spectra using either (a) spin-diffusion or (b) RFDR ^{1}H–^{1}H mixing to establish protein–solvent correlations; the spectra in grey are the corresponding control spectra collected with ^{15}N channel blanked off. The spectra were acquired with 4 transients on a 750 MHz spectrometer with 39 kHz sample spinning rate, for 0.9 μmol protein GB1 that was uniformly ^{2}H, ^{13}C, ^{15}N-enriched, back-exchanged with H_2O and precipitated with methyl-2,4-pentanediol (MPD) and isopropanol (IPA). Relatively weak π pulses with half the nutation frequency of the π/2 ^{1}H pulses are used during RFDR. Recycle delay of 1.5 was used in (a) but 3 s in (b) to reduce duty cycle. Free induction decays were truncated to 14 ms before Fourier transform without apodization.

3.2. Solvent interactions

Water molecules are important for protein structure and function [4]. Also protein samples used in X-ray diffraction or SSNMR are often crystallized with the assistance of other molecules (e.g. polyethylene glycol, MPD, IPA); determining the location of these molecules aids in understanding their role in assisting crystal growth and modulating side-chain structure. Several SSNMR studies on protein–water interactions have been performed nevertheless with only ^{13}C or ^{15}N detection [4,6,7]; proton detection was not used because of the deleterious residual bulk solvent signals. Next we demonstrate that with MISSISSIPPI, it is possible to detect only solvent signals that are transferred from the protein.

Protein and solvent interactions were examined with ^{2}H, ^{13}C, ^{15}N-GB1 (back-exchanged with H_2O), utilizing ^{1}H–^{1}H mixing in the pulse sequence (Fig. 1). Spectra with mixing times from 0 to 100 ms in 1-ms steps were acquired for spin-diffusion (Fig. 3a) and RFDR (Fig. 3b). With increasing mixing time ($\tau_M = 0$, 6, 12, 20, 40 ms; Fig. 3), the solvent signals monotonically increase for spin-diffusion (Fig. 3a) but maximize around 12 ms for RFDR (Fig. 3b). The maximal achievable solvent intensities are much larger in the spin-diffusion than RFDR experiments. It is also obvious that the amide signals decay much faster in the RFDR experiments. Control experiments that have identical parameters in the ^{1}H channel but with ^{15}N channel turned off are also shown in Fig. 3. The control spectra prove that the recovery of bulk solvent signal during the mixing period can be ignored and that the observed solvent intensities in the normal spectra are transferred from the protein.

The decay of amide signal and rise of solvent signals are shown in Fig. 4. These trajectories were fitted with exponential models and the time constants are listed in Table 1. The amide signals decay much slower for spin-diffusion (decay time constant $\tau_d = 63.7$ ms) than for RFDR ($\tau_d = 7.8$ ms). RFDR effectively recouples the dipolar interaction among protons, especially those within the relatively immobile protein molecule. The total signal (integration from 0.9 to 11 ppm) decays extremely slowly for spin-diffusion, with $\tau_d = 0.54$ s agreeing with amide proton T_1 (measured by adding an inversion pulse to the sequence shown in Fig. 1). For RFDR, the total signal decay time constant is only 13.0 ms; the recoupled dipolar interactions expedite the longitudinal relaxation.

The solvent trajectories under spin-diffusion are well fit with a single exponential growth model, with time constant $\tau_g = 26.1$, 30.6 and 33.8 ms for water, alcohol groups and methyl groups, respectively. The decay appears to be dictated by T_1 relaxation, which is at least 10 times slower and not necessary to be included in the fitting model. On the other hand, the trajectories under RFDR mixing re-

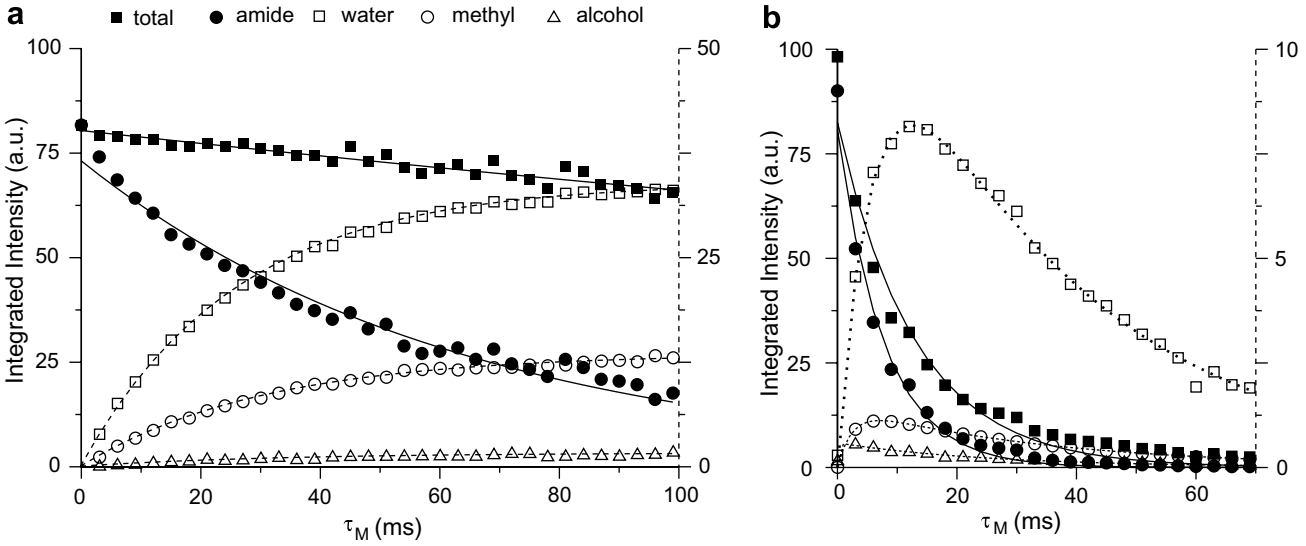

Fig. 4. Trajectories for protein and solvent signals with (a) spin-diffusion and (b) RFDR ^{1}H–^{1}H mixing. The build-up curves (open symbols, right vertical axis) are plotted in a different scale from the decay curves (filled symbols, left axis). The curves for amide protons (integration over 11–6 ppm) and all protons (11–0.9 ppm) were fitted with a single exponential decay model; the curves for water (5.3–4.6 ppm), alcohol (4.3–3.9 ppm) and methyl (1.4–0.9 ppm) signals were fitted with a single exponential growth model in (a) and a dual growth-decay exponential model in (b). Fit parameters are listed in Table 1. Data with a 1-ms time step (τ_M) were acquired and fitted for the curves but only every third point is shown for clarity.

Table 1
Decay (τ_d) and growth (τ_g) time constants of the protein and solvent signals under the influential of spin-diffusion and RFDR ^{1}H–^{1}H mixings

	Spin-diffusion			RFDR		
	A[a]	τ_d (ms)	τ_g (ms)	A[a]	τ_d (ms)	τ_g (ms)
Total	80	538.0	—	82	13.0	—
Amide	73	63.7	—	81	7.8	—
Water	34	—	26.1	14	33.7	7.0
Alcohol	1.6	—	30.6	0.58	25.6	0.003[b]
Methyl	13	—	33.8	1.5	34.0	2.7

[a] Pre-exponential constant for fit.
[b] For this extremely fast growing component, accuracy is limited by the 1-ms step size.

quire both exponential growth and exponential decay fit parameters. The growth time constants are $\tau_g = 7.0$, 0.003 and 2.7 ms and the decay time constant $\tau_d = 33.7$, 25.6 and 34.0 ms for water, alcohol, and methyl, respectively. We attribute the extremely fast initial growth of the alcohol signals to the overlapping Thr hydroxyl protons.

Maximal achievable solvent intensities are significantly higher for spin-diffusion than RFDR from Fig. 4. This can also be seen by comparing the pre-exponential fitting parameter, which corresponds to the saturating intensity in the absence of relaxation. The ratios of pre-exponential parameters are 2.4, 2.8 and 8.7 for water, alcohol and methyl, respectively.

4. Conclusions

We have demonstrated that MISSISSIPPI can achieve very efficient multiple solvent suppression in SSNMR by a combination of homospoil gradients and RF saturation pulses. MISSISSIPPI enables the sensitivity benefit of proton detection to be translated to new, challenging applications. The dynamic range afforded by MISSISSIPPI has allowed 1D spectra to be acquired on natural abundance samples and examination of solvent signals correlated to the protein. We envision that MISSISSIPPI will become a widespread building block in future proton detection SSNMR experiments, including straightforward extensions to additional dimensions for a variety of applications.

Acknowledgments

This work is supported by the National Institutes of Health R01GM75937 (Roadmap Initiative and NIGMS). The authors appreciate technical advice from Charles Mullen, Mircea Cormos, John Stringer and Dennis Sandoz (Varian, Inc.), as well as sample preparation assistance from Gautam Shah.

References

[1] F. Castellani, B.V. Rossum, A. Diehl, M. Schubert, K. Rehbein, H. Oschkinat, Structure of a protein determined by solid-state magic-angle-spinning NMR spectroscopy, Nature 420 (2002) 98–102.
[2] A. Lange, S. Becker, K. Seidel, O. Pongs, M. Baldus, A concept for rapid protein-structure determination by solid-state NMR spectroscopy, Angew. Chem. Int. Ed. 44 (2005) 2089–2092.
[3] S.G. Zech, A.J. Wand, A.E. McDermott, Protein structure determination by high-resolution solid-state NMR spectroscopy: application to microcrystalline ubiquitin, J. Am. Chem. Soc. 127 (2005) 8618–8626.
[4] A. Lesage, A. Böckmann, Water–protein interactions in microcrystalline Crh measured by ^{1}H–^{13}C solid-state NMR spectroscopy, J. Am. Chem. Soc. 125 (2003) 13336–13337.
[5] N. Giraud, J. Sein, G. Pintacuda, A. Böckmann, A. Lesage, M. Blackledge, L. Emsley, Observation of heteronuclear overhauser

effects confirms the ^{15}N–^{1}H dipolar relaxation mechanism in a crystalline protein, J. Am. Chem. Soc. 128 (2006) 12398–12399.
[6] V. Chevelkov, K. Faelber, A. Diehl, U. Heinemann, H. Oschkinat, B. Reif, Detection of dynamic water molecules in a microcrystalline sample of the SH3 domain of α-spectrin by MAS solid-state NMR, J. Biomol. NMR 31 (2005) 295–310.
[7] A. Lesage, L. Emsley, F. Penin, A. Böckmann, Investigation of dipolar-mediated water–protein interactions in microcrystalline Crh by solid-state NMR spectroscopy, J. Am. Chem. Soc. 128 (2006) 8246–8255.
[8] B. Reif, R.G. Griffin, ^{1}H detected ^{1}H, ^{15}N correlation spectroscopy in rotating solids, J. Magn. Reson. 160 (2003) 78–83.
[9] V. Chevelkov, B.J. van Rossum, F. Castellani, K. Rehbein, A. Diehl, M. Hohwy, S. Steuernagel, F. Engelke, H. Oschkinat, B. Reif, ^{1}H detection in MAS solid-state NMR spectroscopy of biomacromolecules employing pulsed field gradients for residual solvent suppression, J. Am. Chem. Soc. 125 (2003) 7788–7789.
[10] E.K. Paulson, C.R. Morcombe, V. Gaponenko, B. Dancheck, R.A. Byrd, K.W. Zilm, Sensitive high resolution inverse detection NMR spectroscopy of proteins in the solid state, J. Am. Chem. Soc. 125 (2003) 15831–15836.
[11] V. Chevelkov, K. Rehbein, A. Diehl, B. Reif, Ultra-high resolution in proton solid-state NMR spectroscopy at high levels of deuteration, Angew. Chem. Int. Ed. 45 (2006) 3878–3881.
[12] D.H. Zhou, J.J. Shea, A.J. Nieuwkoop, W.T. Franks, B.J. Wylie, C. Mullen, D. Sandoz, C.M. Rienstra, Solid-state protein-structure determination with proton-detected triple-resonance 3D magic-angle-spinning NMR spectroscopy, Angew. Chem. Int. Ed. 46 (2007) 8380–8383.
[13] D.H. Zhou, G. Shah, M. Cormos, C. Mullen, D. Sandoz, C.M. Rienstra, Proton-detected solid-state NMR spectroscopy of fully protonated proteins at 40 kHz magic-angle spinning, J. Am. Chem. Soc. 129 (2007) 11791–11801.
[14] W.T. Franks, D.H. Zhou, B.J. Wylie, B.G. Money, D.T. Graesser, H.L. Frericks, G. Sahota, C.M. Rienstra, Magic-angle spinning solid-state NMR spectroscopy of the β1 immunoglobin binding domain of protein G (GB1): ^{15}N and ^{13}C chemical shift assignments and conformational analysis, J. Am. Chem. Soc. 127 (2005) 12291–12305.
[15] C. Ammann, P. Meier, A. Merbach, A simple multinuclear NMR thermometer, J. Magn. Reson. 46 (1982) 319–321.
[16] E.O. Stejskal, J. Schaefer, J.S. Waugh, Magic-angle spinning and polarization transfer in proton-enhanced NMR, J. Magn. Reson. 28 (1977) 105–112.
[17] S. Hediger, B.H. Meier, R.R. Ernst, Adiabatic passage Hartmann–Hahn cross polarization in NMR under magic angle sample spinning, Chem. Phys. Lett. 240 (1995) 449–456.
[18] M. Ernst, A. Samoson, B.H. Meier, Low-power XiX decoupling in MAS NMR experiments, J. Magn. Reson. 163 (2003) 332–339.
[19] A.J. Shaka, J. Keeler, R. Freeman, Evaluation of a new broadband decoupling sequence: WALTZ-16, J. Magn. Reson. 53 (1983) 313–340.
[20] A.E. Bennett, R.G. Griffin, Chemical shift correlation spectroscopy in rotating solids: radio frequency-driven dipolar recoupling and longitudinal exchange, J. Chem. Phys. 96 (1992) 8624–8627.
[21] K. Takegoshi, S. Nakamura, T. Terao, ^{13}C–^{1}H dipolar-assisted rotational resonance in magic-angle spinning NMR, Chem. Phys. Lett. 344 (2001) 631–637.
[22] Y. Ishii, J.P. Yesinowski, R. Tycko, Sensitivity enhancement in solid-state ^{13}C NMR of synthetic polymers and biopolymers by ^{1}H NMR detection with high-speed magic angle spinning, J. Am. Chem. Soc. 123 (2001) 2921–2922.
[23] D.J. States, R.A. Haberkorn, D.J. Ruben, A two-dimensional nuclear overhauser experiment with pure absorption phase in four quadrants, J. Magn. Reson. 48 (1982) 286–292.
[24] D. Marion, M. Ikura, R. Tschudin, A. Bax, Rapid recording of 2D NMR spectra without phase cycling. Application to the study of hydrogen exchange in proteins, J. Magn. Reson. 85 (1989) 393–399.
[25] T. Gullion, D.B. Baker, M.S. Conradi, New, compensated Carr–Purcell sequences, J. Magn. Reson. 89 (1990) 479–484.